Hindawi
Advances in Condensed Matter Physics
Volume 2022, Article ID 1036942, 6 pages
https://doi.org/10.1155/2022/1036942

Research Article

Analogous Atomic and Electronic Properties between V_N and V_NC_B Defects in Hexagonal Boron Nitride

Chang-Youn Moon, Kee-Suk Hong, and Yong-Sung Kim

[1]*Advanced Instrumentation Institute, Korea Research Institute of Standards and Science, Yuseong, Daejon 34113, Republic of Korea*
[2]*Quantum Technology Institute, Korea Research Institute of Standards and Science, Yuseong, Daejon 34113, Republic of Korea*
[3]*Interdisciplinary Materials Measurement Institute, Korea Research Institute of Standards and Science, Yuseong, Daejon 34113, Republic of Korea*

Correspondence should be addressed to Chang-Youn Moon; cymoon@kriss.re.kr

Received 2 September 2021; Revised 9 December 2021; Accepted 9 December 2021; Published 11 January 2022

Academic Editor: Markus R. Wagner

We investigate defect properties in hexagonal boron nitride (hBN) which is attracting much attention as a single photon emitter. Using first-principles calculations, we find that nitrogen-vacancy defect (V_N) has a lower energy structure in C_{1h} symmetry in 1– charge state than the previously known D_{3h} symmetry structure. Noting that carbon has one more valence electron than boron species, our finding naturally points to the correspondence between V_N and V_NC_B defects with one charge state difference between them, which is indeed confirmed by the similarity of atomic symmetries, density of states, and excitation energies. Since V_NC_B is considered as a promising candidate for the source of single photon emission, our study suggests V_N as another important candidate worth attention, with its simpler form without the incorporation of foreign elements into the host material.

1. Introduction

The conventional importance and interest of point defects in solids lie in their impacts on the electrical and optical properties of the material hosts, in which the behavior of a single specific defect has little meaning apart from others. Within more recently emerging quantum technology, on the contrary, the individual defect has significance as a building block of quantum computation [1, 2], quantum cryptography [3, 4], and quantum communication [5]. Recently, single photon emission (SPE) has been discovered [6–9] in hexagonal boron nitride (hBN), characterized by a strong zero-phonon line (ZPL) in the optical spectrum thanks to weak coupling to phonon modes [10]. With desirable properties such as a wide band gap and thermal and chemical stability [11, 12], hBN has become one of the most promising materials for quantum applications.

Besides ZPL at around 2 eV energy, other physical properties relevant to identify the source of SPE include the Huang–Rhys factor related to the electron-phonon coupling strength [10], spin states [13], and the polarization of the optical transition [10, 14]. Depending on their unique evaluation of these properties, different studies have reached different conclusions: a nitrogen vacancy (V_N) [15], boron dangling bonds [16], a complex defect consisting of V_N next to a carbon substitutional replacing a boron atom (V_NC_B) [9, 17–19], V_N adjacent to a nitrogen antisite (V_NN_B) [20, 21], and a boron vacancy next to a carbon substitutional replacing nitrogen (V_BC_N) [22], have been suggested to be promising candidates.

While most of the previous theoretical studies focus on the accurate estimation of excited state properties adopting some advanced methods beyond standard density-functional theory (DFT), the basic ground state energetics seems to have received less attention. For example, it is known that V_NC_B has C_{2v} symmetry with only in-plane atomic displacements, either in the spin singlet [18, 19] or triplet [17] state. A recent study has demonstrated that this structure is

actually unstable against the symmetry-lowering (C_{1h}) relaxation with out-of-plane atomic displacements, consistent with the Stark shift of SPE via an out-of-plane electric field [23]. However, there has not been enough discussions on its physical contents and impact on the validity of previously suggested candidate defects.

In the present study, we revisit the ground state atomic and electronic configurations of some important defect structures using first-principles DFT calculations. After C_{1h} symmetry with out-of-plane relaxation is confirmed as the ground state atomic configuration of the V_NC_B defect, we investigate the possible analogy between V_NC_B and V_N with one more electron. Surprisingly, it is found that 1− charged V_N undergoes the same symmetry lowering relaxation to C_{1h} as neutral V_NC_B. Moreover, neutral V_N and 1+ charged V_NC_B also have similar atomic and electronic configurations as expected. Based on the correspondence between the two defect structures, we suggest V_N as another possible candidate for SPE whose physical properties need to be thoroughly investigated.

Our first-principles calculations are based on DFT with the PAW potential [24, 25] as implemented in the VASP code [26, 27]. The generalized gradient approximation (GGA) of Perdew, Burke, and Ernzerhof (PBE) [28] is adopted for the exchange-correlation functional, facilitating the easier comparison with previous calculational works that also used PBE. Electronic wave functions are expanded with plane waves up to a cutoff energy of 500 eV. A supercell consisting of $6 \times 6 \times 3$ primitive units of hBN is used to ensure minimal spurious interactions among a defect structure and its periodic images. We adopt the experimental lattice constants and internal coordinates are fully relaxed. The K-point sampling is performed on a $2 \times 2 \times 2$ Monkhorst–Pack grid [29].

2. Result and Discussion

First, we investigate the stable atomic structure of V_NC_B, which has been suggested as one of the promising candidates as the source of SPE. As shown in Figure 1(a), the C_{1h} symmetry structure with out-of-plane displacements (0.6 Å for the carbon atom) is found to be the most stable for the neutral charge state in accordance with recent work [23], with no sign of stable spin-polarized solution (i.e., spin-triplet state). When an electron is removed to become 1+ charged state $V_NC_B^{1+}$, it still retains C_{1h} symmetry, but with much reduced out-of-plane displacements (0.2 Å for the carbon atom), as shown in Figure 1(b), which is closer to C_{2v} symmetry than the neutral state. While carbon is a foreign species in the hBN host and its presence naturally breaks the local symmetry, there is also a possibility of spontaneous symmetry breaking in native defects consisting of only host species, boron and nitrogen. Replacing the carbon atom with boron turns V_NC_B to V_N, and we find that the spontaneous symmetry breaking indeed takes place with one of three equivalent boron atoms in a V_N defect displaced out-of-plane direction in C_{1h} symmetry, even in the case of starting the atomic relaxation from the D_{3h} symmetry (i.e., three equivalent boron atoms around missing nitrogen). Since carbon has one more valence electron than boron, we can expect similar properties between V_N and V_NC_B, with the former in one more negatively charged state. In fact, larger out-of-plane atomic displacement of 0.4 Å is found for V_N^{1-}, while it has smaller 0.1 Å displacement in the neutral state V_N^0, as shown in Figures 1(c) and 1(d), respectively.

The correspondence between V_N and V_NC_B defects and the symmetry breaking atomic relaxation can be understood by their electronic structures. Figure 2 shows the density of states (DOS) of the defects in different charge states. For $V_NC_B^{1+}$, only one electron occupies localized defect states, shown as small peaks inside the band gap energy region. The presence of an unpaired electron results in a local magnetic moment of 1 μ_B and our spin-polarized calculation shows that only a spinup state is occupied below the Fermi energy (E_F) while spindown states are above E_F by the exchange splitting, resulting in a spin "doublet" state. The orbital character of the occupied defect level, as represented by a peak around −0.6 eV, is shown in Figure 3(c) as HOMO (highest occupied molecular orbital). The two boron atoms around the missing nitrogen atom form a bond, with the wave function amplitude connecting them, while the carbon atom forms an antibond with them, with vanishing wave function amplitude between the carbon and the two boron atoms. This wave function character can be readily seen in supplemental Figure 5 in [17]. This defect state becomes more stable by decreasing the distance between the two boron atoms in the bonding state while increasing the distance between the carbon and the two boron atoms which are in an antibonding state, which can be facilitated by the out-of-plane relaxation of the carbon atom as the driving force of the symmetry reduction from C_{2v} to C_{1h}. Meanwhile, in the neutral state with two electrons, both spinup and down states are occupied by an electron each, as shown in Figure 2(a), exhibiting a spin "singlet" state. The energy gain by the out-of-plane relaxation of the carbon atom is enhanced by the presence of two electrons compared with the case of only one electron in the 1+ charge state, explaining the enhanced symmetry breaking with the larger out-of-plane displacement of the carbon atom in the neutral state compared with the 1+ charge state as depicted in Figures 1(a) and 1(b). The electronic structure of V_N defect has a close analogy with that of V_NC_B as expected, displayed in Figures 2(c) and 2(d). V_N^0 has one electron as $V_NC_B^{1+}$ does, and hence exhibits the spin doublet configuration. In the case of V_N^{1-}, which has two electrons, same with $V_NC_B^0$, the spin singlet configuration is obtained with the enhanced symmetry breaking out-of-plane atomic displacement, as shown in Figures 1(c) and 1(d). Previously, V_N only in D_{3h} symmetry has been known, and we find that it is 0.14 eV more stable in the C_{1h} symmetry structure for the 1− charged case.

On the other hand, the defect states are overall shifted to higher energies and closer to the bulk conduction states in V_N than in V_NC_B, and this leads to the difference of charge transition levels (CTLs), as depicted in Figure 3(a). For V_NC_B, 1+/0 CTL, which corresponds the position of E_F below (above) which 1+ charge (neutral) state is stabilized, is estimated to be 1.57 eV above the valence band minimum

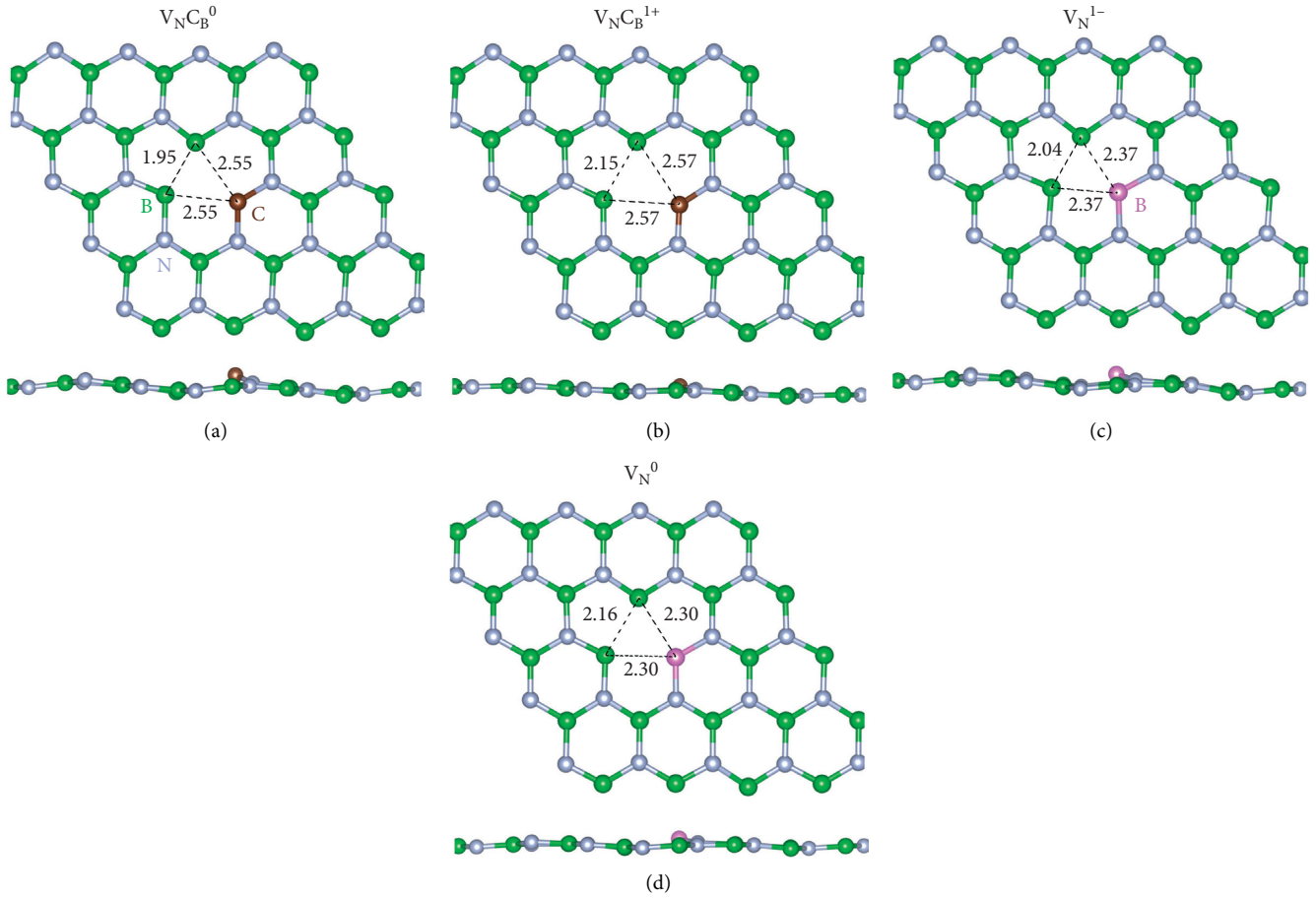

Figure 1: Optimized atomic structures of (a) neutral V_NC_B, (b)V_NC_B in 1+ charge state, (c)V_N in 1− charge state, and (d) neutral V_N. For each defect, the upper structure depicts the view in the out-of-plane direction, while the lower one is the side (in-plane) view. Distances between two atoms around the missing nitrogen atom are displayed in Å unit. In (c) and (d), the boron atom which protrudes out of the plane is shown in a color (pink) different from that of other boron atoms (green).

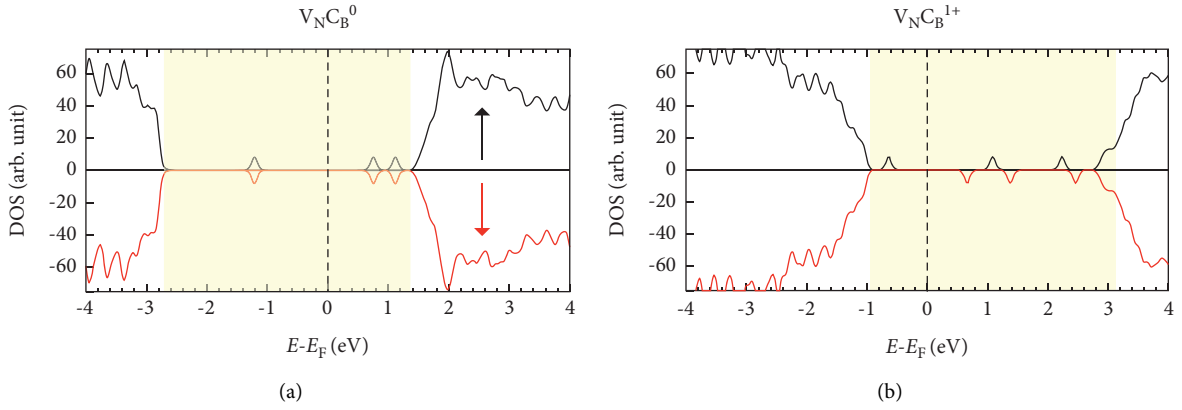

Figure 2: Continued.

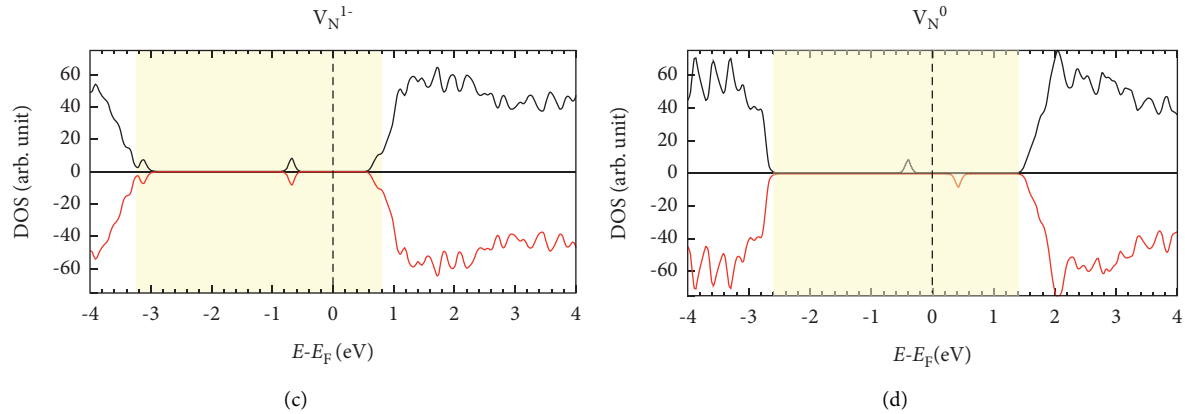

FIGURE 2: Density of states (DOS) of (a) neutral V_NC_B, (b)V_NC_B in 1+ charge state, (c)V_N in 1− charge state, and (d) neutral V_N. Shaded areas represent the bulk band gap energy region, in which small peaks originate from localized defect states. Positive and negative DOS are for spin up and down channels, respectively.

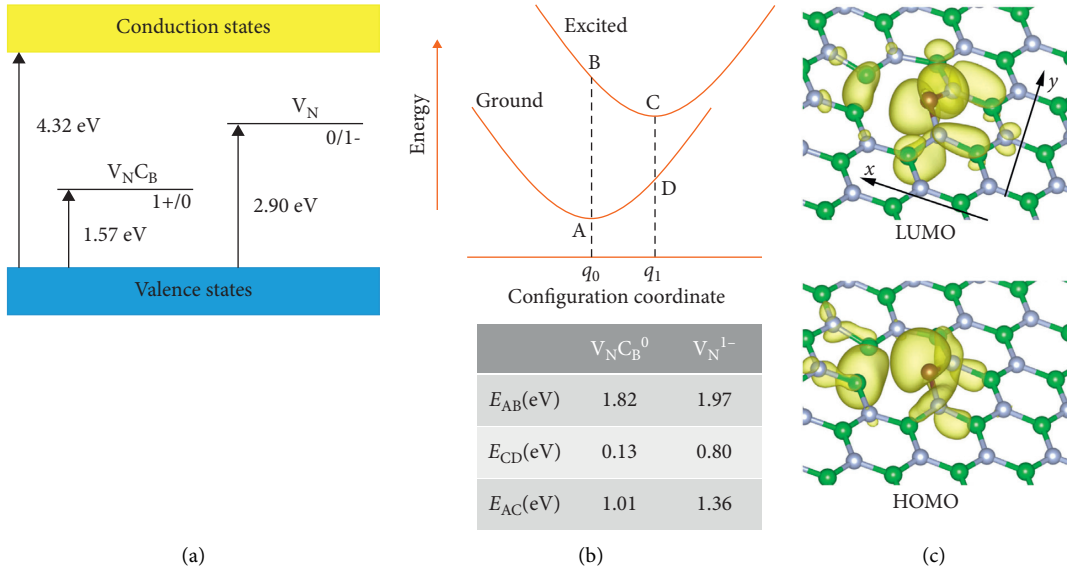

	$V_NC_B^0$	V_N^{1-}
E_{AB}(eV)	1.82	1.97
E_{CD}(eV)	0.13	0.80
E_{AC}(eV)	1.01	1.36

FIGURE 3: (a) Charge transition level (CTL) of defects. For V_NC_B, CTL between 1+ and neutral state is shown while it is between neutral and 1− charge state for V_N, where our calculated band gap is 4.32 eV. (b) Schematic representation of types of the optical transition. The x-axis is for the configuration coordinate which indicates distances among atomic configurations, where q_0 is for the lowest energy atomic configuration of the electronic ground state while q_1 for that of an electronically excited state. In the table, optical absorption (E_{AB}), emission ($E_{C\,D}$), and ZPL (E_{AC}) energies are shown for the two defect structures. (c) Isosurface representation of the squared amplitude of wave functions ($|\psi|^2$) of HOMO and LUMO. The mirror axis of C_{1h} symmetry is chosen as x-direction and its perpendicular direction in the plane of a single atomic layer is along y-axis.

(VBM). Meanwhile, the corresponding 0/1− CTL in V_N is found to be higher, 2.90 eV above VBM. Compared with our GGA band gap of 4.32 eV, $V_NC_B^0$ is stable unless the system is p-doped, whereas V_N^{1-} is stabilized in slightly n-doped samples which can be realized, for example, in oxygen contaminated samples [16]. Noting that $V_NC_B^0$ has been considered as a promising candidate for SPE, now we estimate its optical transition energies by differences between ground and excited states, along with its analogous V_N^{1-}. There are four different configurations of a defect-contained system for which total energies need to be calculated, as schematically depicted in Figure 3(b): the electronic ground state with the relaxed atomic structure (A), the electronically excited state with the atomic structure fixed to that for $A(B)$, the electronically excited state with the atomic structure fully relaxed (C), and the electronic ground state with the atomic structure fixed to that for $C(D)$. The electronically excited state is obtained by holding an electron to the excited Kohn–Sham (i.e., one-electron) state just above the highest occupied defect state while performing the usual self-consistent-field (SCF) ground state calculation. This scheme is often referred to as ΔSCF [30] and was used in many previous calculations [9, 16–18]. Without appropriate band gap correction using techniques such as hybrid functional or GW, this method inevitably tends to underestimate transition energies.

The energy difference between configurations A and B, E_{AB}, corresponds to the absorption energy and $E_{C\,D}$ is the emission energy, both of which do not involve the phonon. E_{AC}, meanwhile, is a ZPL where the electronic transition can take place between different atomic configurations via the overlap of the lowest phonon modes. The ZPL of $V_N C_B^0$ is calculated to be 1.01 eV, as shown in the table in Figure 3(b), which must be underestimated due to the band gap error typical for standard DFT calculations. On the other hand, E_{AC} for V_N^{1-} is found to be 1.36 eV, 0.35 eV larger than that of $V_N C_B^0$. Since previous theoretical studies [9, 17–19] report that the error-corrected ZPL of $V_N C_B^0$ lies within the experimentally observed ZPL range between 1.6 and 2.2 eV [7], the ZPL of V_N^{1-} is also expected to fall in within that energy range assuming that the difference of calculated ZPL between defects does not vary much after the band gap correction. Notably, atomic relaxation energies associated with the electronic excitation (i.e., energy differences between B and C and A and D) are smaller in V_N^{1-}, implying smaller electron-phonon coupling and Huang–Rhys factor. In the meantime, the lower symmetry of defects results in more allowed polarization directions for the optical transition. Figure 3(c) shows the squared amplitude of the highest occupied and lowest unoccupied molecular orbital (HOMO and LUMO, respectively) wave functions in $V_N C_B^0$. HOMO exhibits σ bonding character while LUMO originates from p_z orbital of the carbon atom. In this case, optical transition is allowed for both x and z linear polarization (i.e., $\langle \psi_{\mathrm{LUMO}} | x \text{ or } z | \psi_{\mathrm{HOMO}} \rangle \neq 0$) because both HOMO and LUMO are even functions along the y direction. With planar atomic relaxation only, as in C_{2v} symmetry, the σ-like state would be even while the p_z-like state is odd in the z direction, so that only z-polarized transition would be allowed.

Our work finds a new ground state for one of the most basic native defects, V_N, which has a lower C_{1h} symmetry than the previously known D_{3h} symmetry. We also find a close correspondence between V_N and $V_N C_B$ defects with similar electronic structures and ZPLs. Many former studies, with advanced theoretical methods correcting typical DFT errors, found the properties of $V_N C_B^0$ compatible with experiments. Therefore, our result naturally suggests that V_N^{1-} is another promising candidate for SPE. The fact that electron irradiation [7] or ion implantation [14] increases the formation probability of emitters further supports the plausibility of vacancy defects in general. Moreover, out-of-plane relaxation in V_N^{1-} is also consistent with the Stark effect observed for out-of-plane electric fields [23]. As our calculation results have limitations related to intrinsic DFT errors, further theoretical studies beyond standard DFT are necessary to thoroughly investigate their physical properties. Our result also calls attention to the possibility for symmetry-broken ground states of other defect structures in hBN.

3. Conclusions

In conclusion, we suggest the close analogy between $V_N C_B$ and V_N defects with one charge state difference. Both defect structures with two electrons have C_{1h} symmetry with the spin singlet state and out-of-plane atomic displacements to gain in energy by increasing the distance between atoms in an anti-bonding state, in contrast to previous reports with in-plane displacements only and/or the spin triplet state. ZPL within standard DFT is calculated to be 1.01 and 1.36 eV for $V_N C_B^0$ and V_N^{1-}, respectively. Based on the possibility of $V_N C_B$ as a promising candidate for SPE in hBN as suggested by previous theoretical works, our result points to the necessity for the attention to the analogous V_N defect and for the further investigation with more accurate theoretical schemes overcoming standard DFT errors in the excitation energy evaluation.

Data Availability

The data that support the findings of this study are available from the corresponding author upon reasonable request.

Conflicts of Interest

The authors declare that they have no conflicts of interest.

Acknowledgments

This research was supported by the Basic Science Research Program through the National Research Foundation of Korea (NRF) funded by the Ministry of Science and ICT (2016R1C1B1014715).

References

[1] T. D. Ladd, F. Jelezko, R. Laflamme, Y. Nakamura, C. Monroe, and J. L. O'Brien, "Quantum computers," *Nature*, vol. 464, Article ID 45, 2010.

[2] D. D. Awschalom, L. C. Bassett, A. S. Dzurak, E. L. Hu, and J. R. Petta, "Quantum spintronics: engineering and manipulating atom-like spins in semiconductors," *Science*, vol. 339, Article ID 1174, 2013.

[3] R. Brouri, A. Beveratos, J.-P. Poizat, and P. Grangier, "Photon antibunching in the fluorescence of individual color centers in diamond," *Optics Letters*, vol. 25, Article ID 1294, 2000.

[4] A. Beveratos, R. Brouri, T. Gacoin, A. Villing, J.-P. Poizat, and P. Grangier, "Single photon quantum cryptography," *Physical Review Letters*, vol. 89, Article ID 187901, 2002.

[5] L. Childress, J. M. Taylor, A. S. Sorensen, and M. D. Lukin, "Fault-tolerant quantum communication based on solid-state photon emitters," *Physical Review Letters*, vol. 96, Article ID 070504, 2006.

[6] T. T. Tran, K. Bray, M. J. Ford, M. Toth, and I. Aharonovich, "Quantum emission from hexagonal boron nitride monolayers," *Nature Nanotechnology*, vol. 11, Article ID 37, 2015.

[7] T. T. Tran, C. Elbadawi, D. Totonjian et al., "Robust multicolor single photon emission from point defects in hexagonal boron nitride," *ACS Nano*, vol. 10, Article ID 7381, 2016.

[8] T. T. Tran, C. Zachreson, A. M. Berhane et al., "Quantum emission from defects in single crystal hexagonal boron nitride," *Physical Review Applied*, vol. 5, Article ID 034005, 2016.

[9] S. A. Tawfik, A. Sajid, M. Fronzi et al., "First-principles investigation of quantum emission from hBN defects," *Nanoscale*, vol. 9, Article ID 13575, 2017.

[10] A. L. Exarhos, D. A. Hopper, R. R. Grote, A. Alkauskas, and L. C. Bassett, "Optical signatures of quantum emitters in suspended hexagonal boron nitride," *ACS Nano*, vol. 11, Article ID 3328, 2017.

[11] G. Cassabois, P. Valvin, and B. Gil, "Hexagonal boron nitride is an indirect bandgap semiconductor," *Nature Photonics*, vol. 10, Article ID 262, 2016.

[12] N. Kostoglou, K. Polychronopoulou, and C. Rebholz, "Thermal and chemical stability of hexagonal boron nitride (h-BN) nanoplatelets," *Vacuum*, vol. 112, Article ID 42, 2015.

[13] A. L. Exarhos, D. A. Hopper, R. N. Patel, M. W. Doherty, and L. C. Bassett, "Magnetic-field-dependent quantum emission in hexagonal boron nitride at room temperature," *Nature Communications*, vol. 10, Article ID 222, 2019.

[14] S. Choi, T. T. Tran, C. Elbadawi et al., "Engineering and localization of quantum emitters in large hexagonal boron nitride layers," *ACS Applied Materials and Interfaces*, vol. 8, Article ID 29642, 2016.

[15] J. R. Toledo, D. B. de Jesus, M. Kianinia et al., "Electron paramagnetic resonance signature of point defects in neutron-irradiated hexagonal boron nitride," *Physical Review B: Condensed Matter*, vol. 98, Article ID 155203, 2018.

[16] M. E. Turiansky, A. Alkauskas, L. C. Bassett, and C. G. Van de Walle, "Dangling bonds in hexagonal boron nitride as single-photon emitters," *Physical Review Letters*, vol. 123, Article ID 127401, 2019.

[17] F. Wu, A. Galatas, R. Sundararaman, D. Rocca, and Y. Ping, "First-principles engineering of charged defects for two-dimensional quantum technologies," *Physical Review Materials*, vol. 1, Article ID 071001, 2017.

[18] A. Sajid, J. R. Reimers, and M. J. Ford, "Defect states in hexagonal boron nitride: assignments of observed properties and prediction of properties relevant to quantum computation," *Physical Review B: Condensed Matter*, vol. 97, Article ID 064101, 2018.

[19] A. Sajid and K. S. Thygesen, "VNCB defect as source of single photon emission from hexagonal boron nitride," *2D Materials*, vol. 7, Article ID 031007, 2020.

[20] A. Sajid, J. R. Reimers, R. Kobayashi, and M. J. Ford, "Theoretical spectroscopy of the V N N B defect in hexagonal boron nitride," *Physical Review B: Condensed Matter*, vol. 102, Article ID 144104, 2020.

[21] S. Gao, H.-Y. Chen, and M. Bernardi, "Radiative properties of quantum emitters in boron nitride from excited state calculations and Bayesian analysis," *NPJ Computational Materials*, vol. 7, Article ID 85, 2021.

[22] N. Mendelson, D. Chugh, J. R. Reimers et al., "Identifying carbon as the source of visible single-photon emission from hexagonal boron nitride," *Nature Materials*, vol. 20, Article ID 321, 2021.

[23] G. Noh, D. Choi, J.-H. Kim et al., "Stark tuning of single-photon emitters in hexagonal boron nitride," *Nano Letters*, vol. 18, Article ID 4710, 2018.

[24] P. E. Blochl, "Projector augmented-wave method," *Physical Review B: Condensed Matter*, vol. 50, Article ID 17953, 1994.

[25] G. Kresse and J. Joubert, "From ultrasoft pseudopotentials to the projector augmented-wave method," *Physical Review B: Condensed Matter*, vol. 59, Article ID 1758, 1999.

[26] G. Kresse and J. Furthmuller, "Efficiency of ab-initio total energy calculations for metals and semiconductors using a plane-wave basis set," *Computational Materials Science*, vol. 6, Article ID 15, 1996.

[27] G. Kresse and J. Furthmuller, "Efficient iterative schemes for ab initio total-energy calculations using a plane-wave basis set," *Physical Review B: Condensed Matter*, vol. 54, Article ID 11169, 1996.

[28] J. P. Perdew, K. Burke, and M. Ernzerhof, "Generalized Gradient Approximation Made Simple," *Physical Review Letters*, vol. 77, Article ID 3865, 1996.

[29] H. J. Monkhorst and J. D. Pack, "Special points for Brillouin-zone integrations," *Physical Review B: Condensed Matter*, vol. 13, Article ID 5188, 1976.

[30] R. O. Jones and O. Gunnarsson, "The density functional formalism, its applications and prospects," *Reviews of Modern Physics*, vol. 61, Article ID 689, 1989.